ACS OMEGA

http://pubs.acs.org/journal/acsodf

Article

Multiscale Screening of Deep Eutectic Solvents for Efficient Extraction of *m*-Cresol from Model Coal Tar

Qian Liu and Xianglan Zhang*

Cite This: *ACS Omega* 2022, 7, 34485−34494

Read Online

ACCESS | Metrics & More | Article Recommendations | Supporting Information

ABSTRACT: Screening of suitable deep eutectic solvents (DESs) as extractants is vitally important in an extraction process. In this study, a multiscale method combining conductor-like screening model for real solvents (COSMO-RS) calculation, experimental validation, and process simulation is presented. This method was applied to screen DESs for extracting *m*-cresol from cumene. First, the COSMO-RS model was performed to calculate the phase equilibrium of different ternary systems at different feed compositions, thereby prescreening DESs by investigating the effects of DES structures on the extraction performance. Then, the prescreened DESs were studied by extraction experiments to further validate their extraction performance. The extraction mechanism was investigated through FT-IR characterization. Afterward, continuous process simulation by Aspen Plus was employed to identify more promising DESs. The COSMO-RS calculation and experimental results showed that both choline chloride (ChCl)/ethylene glycol (EG) (1:2) and ChCl/glycerol (Gly) (1:2) demonstrated a high extraction performance, which were selected as two suitable DESs. Considering the mass purity and recovery ratio of *m*-cresol and cumene products in industrial applications, as well as the extractant dosage and equipment costs, ChCl/Gly (1:2) is considered a more promising DES in industrial application.

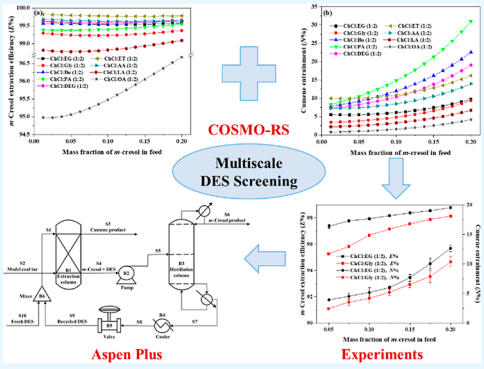

1. INTRODUCTION

Low-temperature coal tar (LTCT) is an additional chemical generated by coal coking at low temperatures.[1] LTCT distillates generally have phenolic compound contents of 20−30 wt %.[2] Phenolic compounds can be used to synthesize a variety of organic chemicals.[3] Moreover, removal of phenols is helpful in increasing the storage stability of oil products and reducing the hydrogen consumption of subsequent processing.[4,5] The extraction is regarded as an effective method for separating phenols from LTCT.[6] It is significant to select a suitable extractant in the extraction process. Conventional solvents (e.g., ethylene glycol and urea) were reported to extract phenols from aromatic or aliphatic hydrocarbons.[7,8] However, their low extraction performances are unfavorable to the extraction process.

Ionic liquids (ILs) as green solvents have been applied in extracting phenols from model coal tar.[9−12] ILs demonstrate the advantages of low flammability, non-toxicity, biodegradability, and so on.[13] Compared with ILs, deep eutectic solvents (DESs) are of low-cost and easily synthesized, which have a broader application prospect.[14−19] For instance, Yi et al. adopted a ChCl (choline chloride)-based DES to extract phenolic compounds.[20] The extraction efficiency (*E*) of *m*-cresol was as high as 98.3%, while the cumene entrainment was only 4.2%. In addition, the DES also demonstrated efficient extraction performance in LTCT distillates. However, a large number of DESs may exist potentially due to the combinations of different hydrogen bond acceptors (HBAs) and hydrogen bond donors (HBDs). Therefore, a rational and efficient DES screening method is highly required.

Extraction experiments and ab initio methods could be applied to screen DESs.[21,22] However, these methods are impractical to evaluate each DES from numerous DES candidates. The classical activity coefficient models can be used to calculate the thermodynamic properties of DESs.[23] However, these models are missing for the binary interaction parameters of new DESs, and the predictive ability of these models for new systems is insufficient. The universal quasichemical functional−group activity coefficients (UNIFAC) model has promoted the predictive ability of extractant screening.[24] Recently, the missing parameters of the UNIFAC-IL model were filled by a neural recommender system.[25] Nevertheless, the UNIFAC model has not been reported in the screening and design of mixtures. Besides, the deep learning model can be used to predict the thermodynamic properties of solvents.[26−29] However, the deep learning model is restricted to investigate systems lacking experimental data.

Received: July 6, 2022
Accepted: September 1, 2022
Published: September 12, 2022

https://doi.org/10.1021/acsomega.2c04234
ACS Omega 2022, 7, 34485−34494

Compared with the abovementioned methods, the conductor-like screening model for real solvents (COSMO-RS) can calculate the thermodynamic properties of pure components and mixtures independent of the experimental data.[30−34] COSMO-RS showed relatively high accuracy in the qualitative and quantitative predictions of thermodynamic properties, which has been widely applied as an efficient DES screening model in different separation systems.[35−39] Nevertheless, the infinite dilution distribution coefficient and selectivity are chosen as screening indicators in the abovementioned works. These two indexes were incapable of investigating the effect of different feed compositions on the separation performance of DESs in a practical system.[40] To improve screening indicators, Cheng et al. employed the distribution coefficient and selectivity at the specific feed composition to screen DESs for extractive desulfurization (EDS).[41] Tetrabutylphosphonium bromide/dimethylformamide (1:3) was identified as the most promising DES for EDS due to its highest distribution coefficient.

For LTCT systems, the phenol E is a common criterion to evaluate the extraction performance of extractants.[42−44] However, this index cannot reflect the oil loss and the phenol purity. The neutral oil entrainment (N) should also be given more attention.[20] Hence, the E and N values calculated from the phase equilibrium of the DES-containing system at different feed compositions are more instructive for screening DESs. Except for the thermodynamic extraction performance based on COSMO-RS, the process performance of extractants is of great significance.[45] Continuous process simulation can identify more promising extractants.[40,46] Nevertheless, it is unrealistic to directly screen extensive DESs through process simulation because the physical parameters and interaction parameters of DESs are missing in the database. Consequently, the combinatorial screening method based on different scales is highly meaningful.

In this study, a multiscale screening method, combining COSMO-RS calculation, experimental evaluation, and process simulation, was used to screen DESs for extracting *m*-cresol from cumene. First, the COSMO-RS model was applied to evaluate the extraction performance at different feed compositions originating from the phase equilibrium for preliminary screening of DESs. Second, the prescreened DESs were validated by extraction experiments to ensure their high separation performance, and the extraction mechanism was investigated by FT-IR characterization. Third, the process performance of the prescreened DESs was evaluated by Aspen Plus. This method initiates from the molecular scale to the single-stage equilibrium scale and then to the engineering scale, which is more reasonable for screening DESs.

2. RESULTS AND DISCUSSION

2.1. COSMO-RS Calculations. In this study, *m*-cresol and cumene are selected as the representative phenolic compound and neutral oil in LTCT, respectively. The feasibility of *m*-cresol/cumene separation is analyzed by the σ-profile.[39] As illustrated in Figure 1, both *m*-cresol and cumene have obvious peaks in the nonpolar region, which mainly correspond to their benzene ring. Unlike cumene, *m*-cresol has a phenolic hydroxyl group, and its σ-profile exhibits peaks at − 0.016 and 0.013 e·Å^{-2}, respectively, indicating its HBD ability and HBA ability, respectively. The difference in σ-profiles provides a feasibility for separating *m*-cresol and cumene.

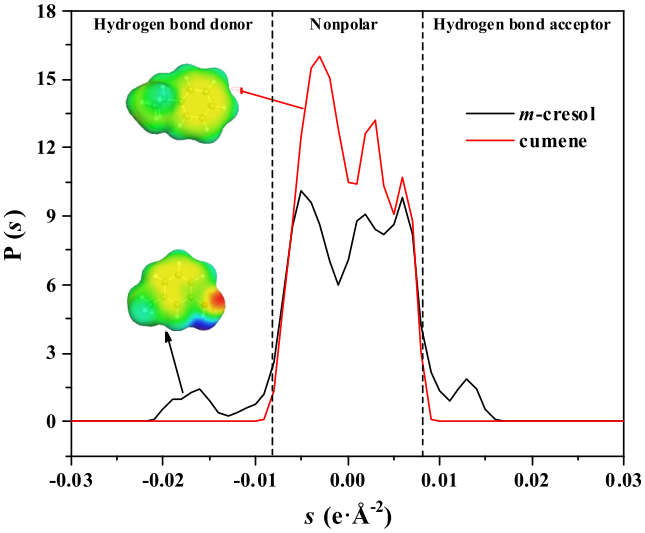

Figure 1. σ-Profiles of *m*-cresol and cumene.

To avoid the massive calculation caused by various combinations, the effects of representative HBAs, HBDs, and molar ratios were studied, respectively. Nine quaternary ammonium salts were selected as HBAs, including choline chloride (ChCl), choline bromide (ChBr), chlorocholine chloride (CChC), acetylcholine chloride (ATCC), tetramethylammonium chloride (TMAC), tetraethylammonium chloride (TEAC), tetrapropylammonium chloride (TPAC), tetraethylammonium bromide (TEAB), and tetraethylphosphonium chloride (TEPC), which had different cations and anions. Nine solvents were chosen as HBDs, including alcohols [i.e., ethylene glycol (EG), glycerol (Gly), 1,2-butanediol (Bu), benzyl alcohol (PA), and diethylene glycol (DEG)], alcohol amine (i.e., monoethanolamine, ET), and carboxylic acids [i.e., acetic acid (AA), lactic acid (LA), and oxalic acid (OA)]. The HBA/HBD molar ratios were investigated from 1:2 to 1:7. The detailed information of the studied HBAs and HBDs is shown in Table S1 (Supporting Information). The mass fraction of model coal tar and DES in the feed was set at 0.5.

2.1.1. Effect of HBA Structure. When studying the effect of HBA types on the DES performance, EG is chosen as the HBD and HBA/HBD is set to 1:2. The E and N of various HBA/EG (1:2) DESs are presented in Figure 2, and the mass ratio of cumene to *m*-cresol in the DES phase (MR) of various HBA/EG (1:2) DESs is also shown in Figure S1 (Supporting Information). For TMAC, TEAC, and TPAC, when the alkyl chain length increases, the DESs exhibit similar E at specific feed compositions, while their N significantly increases. This suggests that when paired with EG at 1:2, the HBA with shorter alkyl chain length can achieve the higher separation performance. For different central atoms of cations, the E of TEPC is similar to that of TEAC, while the N of TEPC is higher than that of TEAC. The choline-based DESs (i.e., ChCl, CChC, and ATCC) have slightly lower E values and obviously lower N values than other DESs. Taking *m*-cresol feed of 0.15 as an example, the E values of ChCl/EG (1:2), CChC/EG (1:2), ATCC/EG (1:2), and TEAC/EG (1:2) are 99.54, 99.22, 99.47 and 99.80%, respectively, while their N values are 7.41, 5.54, 8.60, and 35.40%, respectively. Moreover, DESs with bromide anion demonstrate both relatively lower E and N values than the chloride anion. The same variations of HBA/

https://doi.org/10.1021/acsomega.2c04234
ACS Omega 2022, 7, 34485−34494

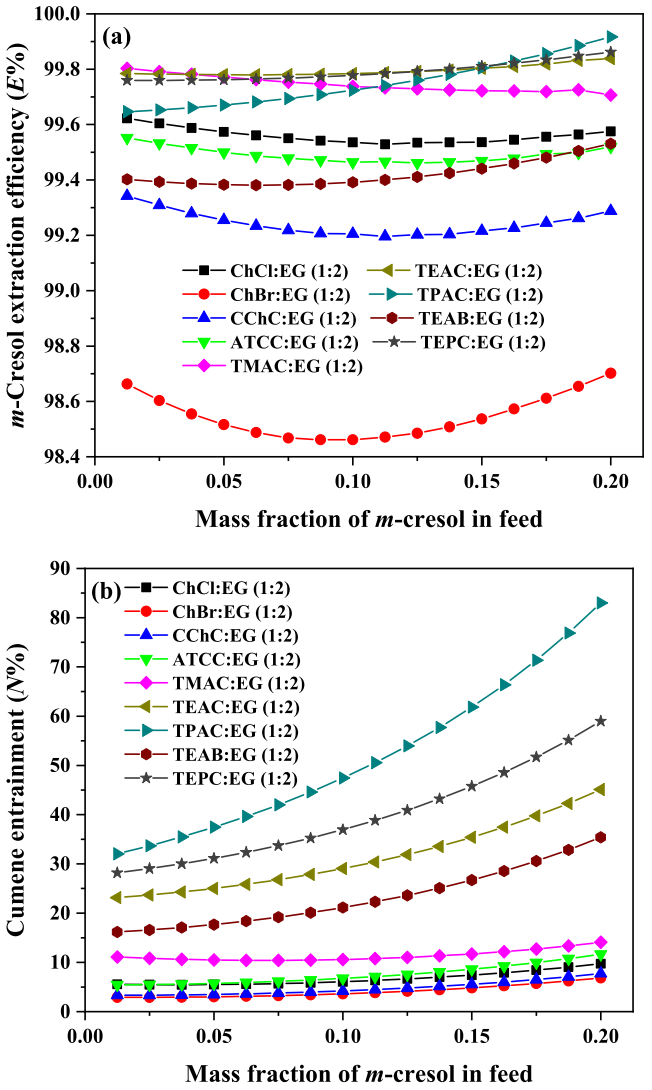

Figure 2. COSMO-RS-calculated E (a) and N (b) of different EG-based DESs at different feed compositions.

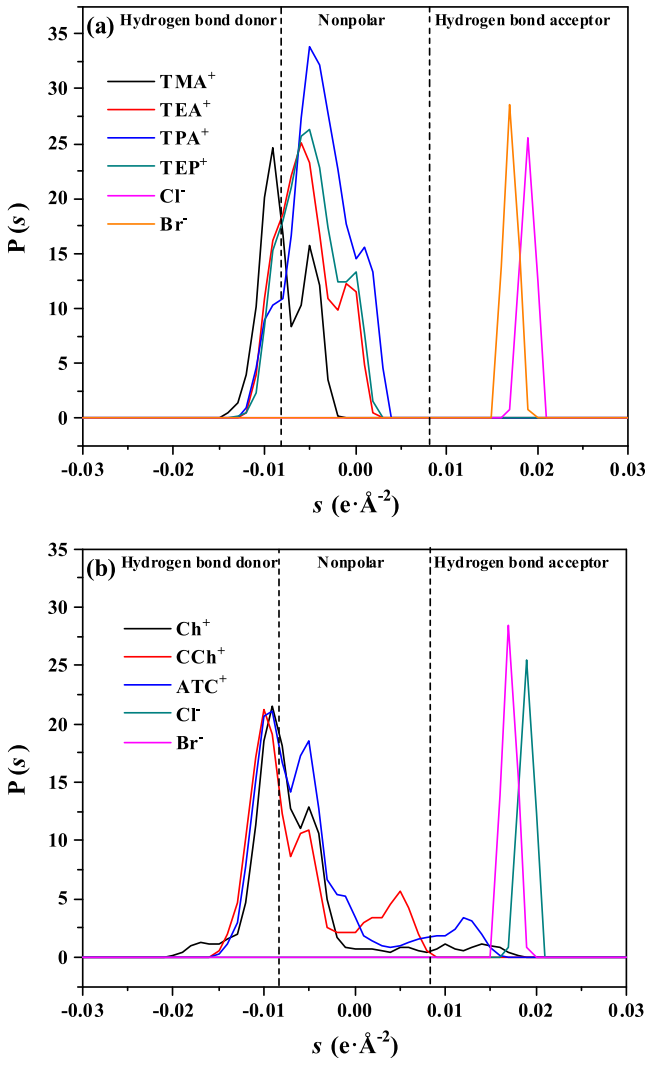

Figure 3. σ-Profiles of TMA^+, TEA^+, TPA^+, TEP^+, Cl^-, and Br^- (a); σ-profiles of Ch^+, CCh^+, ATC^+, Cl^-, and Br^- (b).

Gly (1:2) and HBA/LA (1:2) DESs are observed in Figures S2 and S3 (Supporting Information).

To analyze the effect of HBA structures on the extraction performance, the σ-profiles of different cations and anions in HBA are shown in Figure 3. As is seen, for TMA^+, TEA^+, and TPA^+, as the chain length of cationic alkyl increases, the distribution of their σ-profiles in the nonpolar region gradually increases, suggesting that the non-polarity order of the three cations is as follows: $TPA^+ > TEA^+ > TMA^+$. Considering the strong polarity of m-cresol, the change in the cation chain length has no obvious effect on the E value. For cumene, its σ-profile is mainly distributed in the nonpolar region. Therefore, the N values of DESs gradually increase with increasing alkyl chain length of cation. Similarly, TEP^+ demonstrates a higher peak in the nonpolar region than TEA^+, indicating the higher N value of TEP^+. For Ch^+, CCh^+, and ATC^+, their σ-profiles have small peaks distributed in the HBD region, suggesting their stronger polarity than quaternary ammonium cations. Therefore, the Ch-based, CCh-based, and ATC-based DESs present lower N values than quaternary ammonium-based DESs. Nevertheless, their σ-profiles presented in the nonpolar region are little, resulting in lower E values.

The effect of anions on extraction performance of DESs is also studied through σ-profile analysis, and the results are shown in Figure 3. The σ-profile of Cl^- and Br^- presents obvious peaks at 0.019 and 0.017 e·Å^{-2}, respectively, suggesting that Cl^- presents a stronger HBA ability than Br^-. Hence, DES-containing Cl^- exhibits stronger interaction with m-cresol than DES-containing Br^-, leading to a higher E value. Besides, compared with Br^-, Cl^- is more likely to interact with the HBD, which causes the stronger interaction between cation and cumene. Thus, DES-containing Cl^- has a relatively higher N value.

Furthermore, when the mass fraction of m-cresol in the feed increases, the E value of ChCl/EG (1:2), ChBr/EG (1:2), CChC/EG (1:2), and ATCC/EG (1:2) first decreases and then increases, while the E value of TEAC/EG (1:2), TPAC/EG (1:2), TEAB/EG (1:2), and TEPC/EG (1:2) gradually increases, and the E value of TMAC/EG (1:2) gradually decreases. This is mainly related to the structure of cations in the HBA. From Figure 3, DESs containing similar σ-profiles of cations exhibit similar change trend with increasing mass fraction of m-cresol in the feed. In summary, DESs with ChCl show relatively high E and relatively low N in the meantime. Therefore, ChCl is selected as the HBA candidate.

https://doi.org/10.1021/acsomega.2c04234
ACS Omega 2022, 7, 34485−34494

2.1.2. Effect of HBD Structure. The *E*, *N*, and *MR* of nine ChCl/HBD (1:2) DESs are presented in Figure S4 (Supporting Information). With the increase of the *m*-cresol feed composition from 0.0125 to 0.2, the *E* value of ChCl/OA (1:2) increases from 94.98 to 96.68%, and the *E* values of other DESs have no obvious change. For all DESs, they present low *N* values when the *m*-cresol feed is low. Although DESs with OA and LA as the HBD have lower *N* values than other DESs, their *E* values are significantly lower. For DESs with HBDs of EG, Gly, Bu, PA, DEG, ET, and AA, they all show a high *E* value, indicating the satisfactory extraction performance of *m*-cresol. ChCl/PA (1:2) exhibits the highest *N* due to the strong $\pi-\pi$ bond between PA and cumene.

The σ-profiles of nine HBDs are shown in Figures S5 (Supporting Information). As is seen, the σ-profile of OA has the highest peak in the HBA region, suggesting the strongest HBA ability of OA, which increases the repulsive interaction with *m*-cresol also demonstrating strong HBA ability. On the other hand, the strong polarity of OA also reduces the interaction between OA and cumene. Therefore, OA-based DESs show the lowest *E* and *N* values at the same time. For Bu, PA, and DEG, their σ-profiles present larger peaks in the nonpolar region, indicating that Bu, PA, and DEG have stronger interaction with cumene, resulting in higher *N* values. In order to obtain relatively high *E* and relatively low *N* at the same time, EG and Gly are identified as the suitable HBD.

2.1.3. Effect of Molar Ratio of HBA to HBD. The effects of ChCl/EG and ChCl/Gly molar ratio on the DES performance are studied and are demonstrated in Figures S6 and S7 (Supporting Information), respectively. With changing ChCl/EG and ChCl/Gly from 1:2 to 1:7, the *E* of DESs decreases gradually at specific feed compositions. The *N* of DESs with a molar ratio of 1:2 changes more gently than other molar ratios. Taking ChCl/EG DESs as an example, when the *m*-cresol feed is 0.0125, the *N* values of DESs with the molar ratio from 1:2 to 1:7 are 5.55, 3.99, 3.53, 3.41, 3.41 and 3.47%, respectively. When the *m*-cresol feed is 0.2, their *N* values are 9.73, 10.45, 11.46, 12.51, 13.47, and 14.33%, respectively. Overall consideration, DESs with HBA/HBD of 1:2 demonstrate good separation performance because of the highest *E* and relatively low *N* at specific feed compositions.

2.2. Extraction Experiments. *2.2.1. Evaluation of DESs with Different Molar Ratios on the Extraction Performance.* The *E* and *N* of ChCl/EG and ChCl/Gly DESs with different molar ratios determined by extraction experiments and calculated by COSMO-RS are demonstrated in Figure 4, while the *MR* of ChCl/EG and ChCl/Gly DESs is shown in Figure S8 (Supporting Information). As is seen, when the *m*-cresol feed is 0.15, as the ChCl/EG molar ratio changes from 1:2 to 1:7, both the experimental *E* value and COSMO-RS-calculated *E* value decrease slightly. For example, when the ChCl/EG molar ratio is 1:2, experimental *E* and COSMO-RS-calculated *E* values are 98.90 and 99.54%, respectively, while their *E* values are 97.99 and 98.43% at a ChCl/EG molar ratio of 1:7, respectively. Meanwhile, both the experimental *N* value and COSMO-RS-calculated *N* value increase gradually as the molar ratio varies from 1:2 to 1:7. The variety of *N* values might be due to the fact that when the content of EG in ChCl/EG DES is higher, the *E* value is reduced and leftover *m*-cresol promotes cumene dissolution in the DES via an intermolecular interaction. The similar tendency of ChCl/Gly DESs at different molar ratios can be observed in Figure 4b. As is seen, both the *E* and *N* of ChCl/Gly DESs determined by

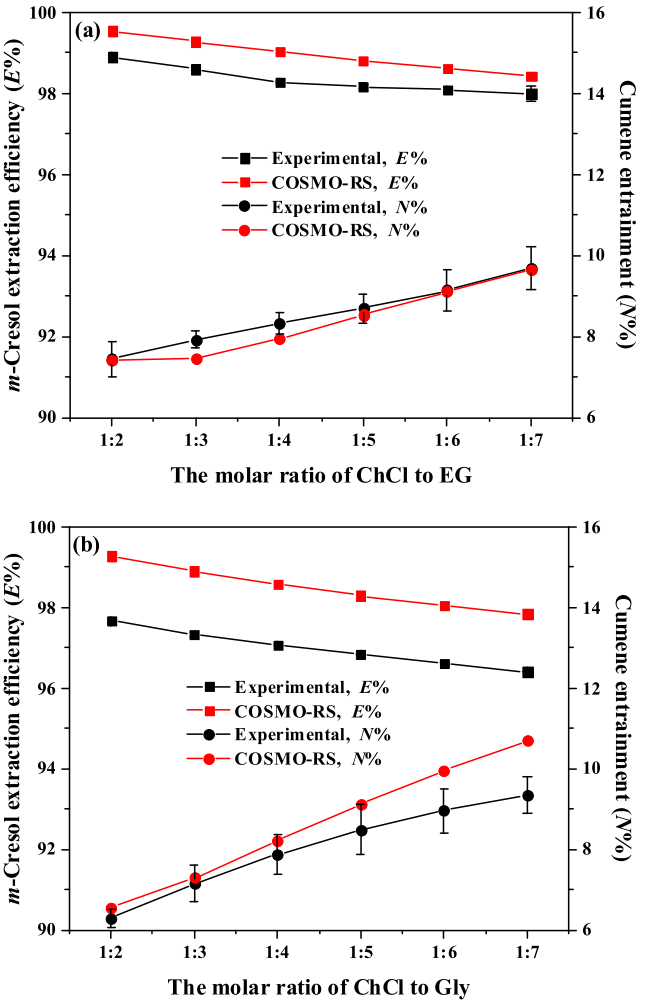

Figure 4. *E* and *N* for different molar ratios of ChCl/EG DESs (a) and ChCl/Gly DESs (b) obtained by experiments and COSMO-RS calculations.

experiments are slightly lower than those calculated by COSMO-RS. ChCl/Gly (1:2) exhibits the highest *E* and the lowest *N* in ChCl/Gly DESs. Hence, HBA/HBD of 1:2 is selected as the optimal molar ratio. ChCl/EG (1:2) and ChCl/Gly (1:2) are identified as suitable extractants to extract *m*-cresol from cumene.

2.2.2. Evaluation of DESs at Different Feed Compositions on the Separation Performance. The *E* and *N* of the identified DESs at different feed compositions determined by extraction experiments and calculated by COSMO-RS are illustrated in Figure 5, while the *MR* of the identified DESs at different feed compositions is shown in Figure S9 (Supporting Information). For both DESs, with increasing *m*-cresol feed, both their experimental *E* and *N* rise gradually. Their COSMO-RS-calculated *E* values are slightly higher than those determined by experiments. The change of experimental *N* values is more evident than COSMO-RS-calculated *N* values as the *m*-cresol feed rises from 0.05 to 0.2. Besides, experimental results indicate that ChCl/EG (1:2) demonstrates higher *E* and *N* values than ChCl/Gly (1:2) at different feed compositions. Both experiments and COSMO-RS calculations show consistent trends of changes. For example, the experimental *E* and *N* of ChCl/EG (1:2) at a *m*-cresol mass fraction in the feed of 0.15 are 98.37 and 7.70%,

https://doi.org/10.1021/acsomega.2c04234
ACS Omega 2022, 7, 34485−34494

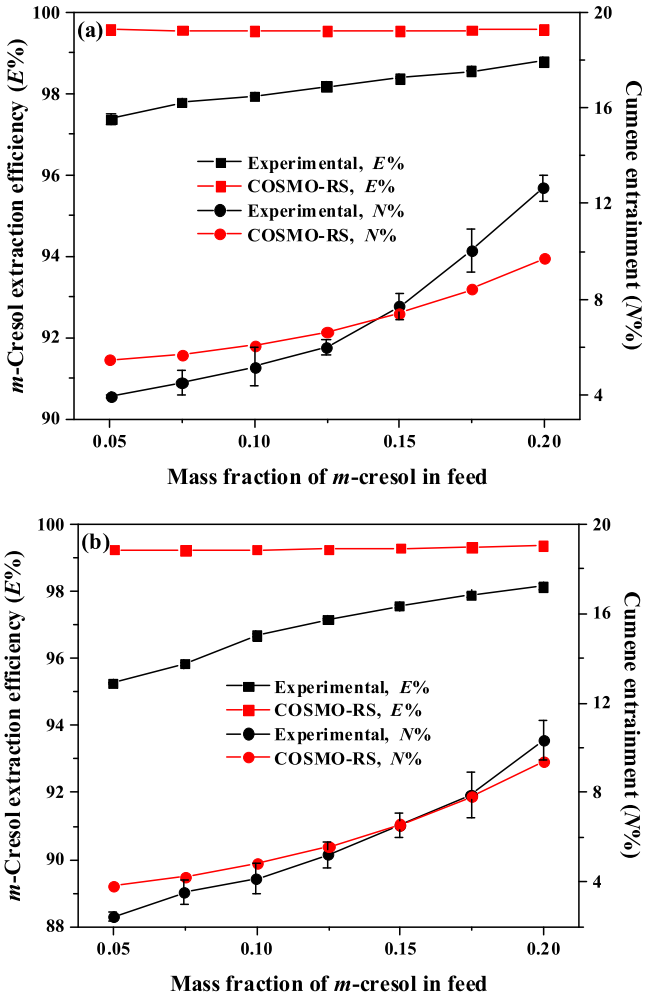

Figure 5. Experimental and COSMO-RS-calculated E and N of ChCl/EG (1:2) (a) and ChCl/Gly (1:2) (b) at different m-cresol feed compositions.

respectively, while these values of ChCl/Gly (1:2) are 97.55 and 6.51%, respectively. At the same feed composition, the COSMO-RS-calculated E and N of ChCl/EG (1:2) are 99.54 and 7.41%, respectively, while these values of ChCl/Gly (1:2) are 99.27 and 6.56%, respectively. Overall, COSMO-RS is an effective research method to quickly evaluate the influence of HBA and HBD compositions on extraction performances of DESs.

2.2.3. Extraction Mechanism Analysis. The extraction mechanism analysis can interpret the interaction between DESs and m-cresol. In addition, this provides guidance for the design of new DESs. FT-IR is a useful technique to identify the hydrogen bond.[47] As seen in Figure 6, the ν-OH stretching vibration of m-cresol shifts from 3312 to 3259 cm^{-1} after interaction between ChCl/EG (1:2) and m-cresol. This value shifts to 3283 cm^{-1} after interaction between ChCl/Gly (1:2) and m-cresol. A larger chemical shift can be observed after the interaction between ChCl/EG (1:2) and m-cresol, suggesting that the ability to form hydrogen bonds for ChCl/EG (1:2) is stronger than that for ChCl/Gly (1:2). Hence, using ChCl/EG (1:2) as the extractant demonstrates a higher E value than that using ChCl/Gly (1:2) in extraction experiments. Moreover, the σ-potential analysis can also be used to understand the extraction mechanism, and the results are shown in Figure S10 (Supporting Information).

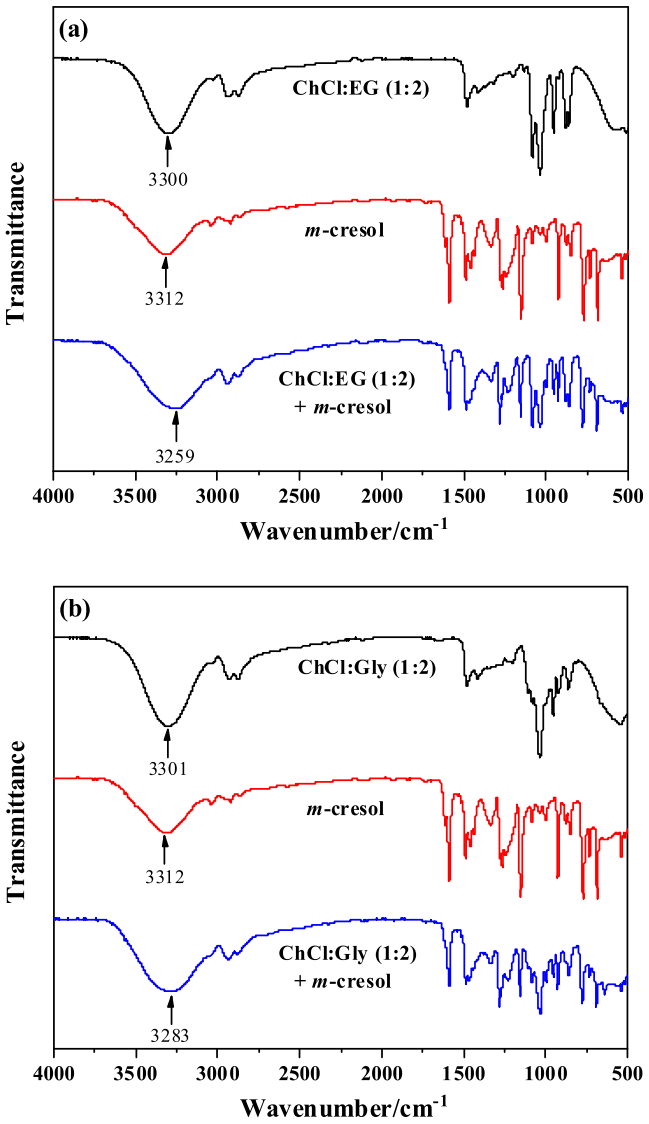

Figure 6. FT-IR spectra of DES, m-cresol, and DES + m-cresol mixture: (a) ChCl/EG (1:2); (b) ChCl/Gly (1:2).

2.3. Process Simulation and Evaluation. Significantly, the extraction experiments are based on the single-stage equilibrium scale. From the perspective of practical industrial applications, continuous process simulation based on the engineering scale can be used to identify more promising DESs. To investigate the operating conditions of the extraction process by DESs, ChCl/EG (1:2) and ChCl/Gly (1:2) are studied for further process simulation.

2.3.1. Parameters of DESs. The required parameters for defining DESs as pseudocomponents are calculated from the literature.[48−50] This DES definition method has been presented to be reliable for simulating DES-based processes of tetralin/dodecane extractive separation and ethanol/water extractive distillation.[51,52] The results are presented in Table S2 (Supporting Information). The liquid−liquid equilibrium (LLE) data from COSMO-RS calculation and non-random two liquids (NRTL) regression are listed in Table S3 (Supporting Information). The root-mean-square deviation (rmsd) is applied to evaluate the consistency between the COSMO-RS-calculated and NRTL-correlated LLE data, which is determined by

https://doi.org/10.1021/acsomega.2c04234
ACS Omega 2022, 7, 34485−34494

Table 1. NRTL Parameters and rmsds for {DES + *m*-Cresol + Cumene} Ternary Systems

component	NRTL parameters (K)					rmsd
i-j	a_{ij}	a_{ji}	b_{ij}	b_{ji}	c_{ij}	
			{ChCl/EG (1:2) (1) + *m*-Cresol (2) + Cumene (3)}			
1-2	−0.46	−1.68	3045.37	−444.05	0.3	0.0153
1-3	6.04	−11.87	−853.40	5745.20	0.2	
2-3	51.63	−6.55	10000.00	2253.13	0.3	
			{ChCl/Gly (1:2) (1) + *m*-Cresol (2) + Cumene (3)}			
1-2	10.73	−1.19	−1056.25	−620.41	0.3	0.0180
1-3	5.48	−7.78	−682.30	4463.32	0.2	
2-3	65.32	−6.67	10000.00	2312.80	0.3	

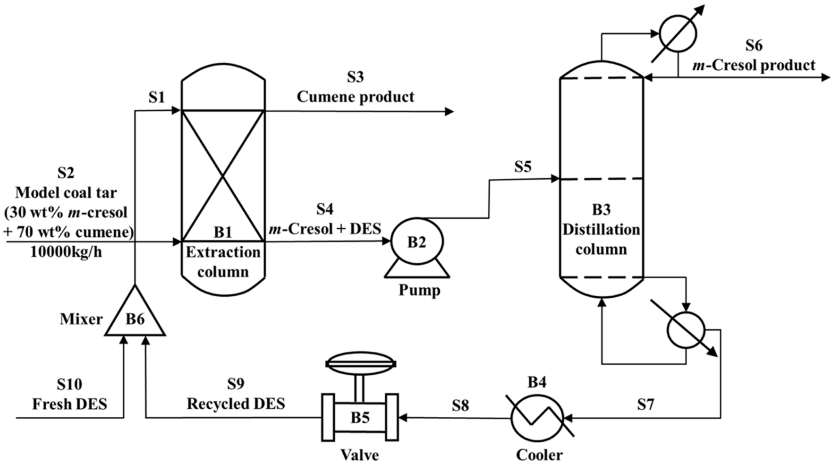

Figure 7. Continuous extraction process for extracting *m*-cresol from cumene with DESs as the extractant.

$$\text{rmsd} = \left\{ \sum_i \sum_l \sum_m (w_{ilm}^{\text{cal}} - w_{ilm}^{\text{cor}})^2 / 6N_t \right\}^{1/2} \quad (1)$$

where the subscripts i, l, and m represent the component, the phase, and the tie-line, respectively, N_t refers to the total number of tie-lines, w^{cal} and w^{cor} are the COSMO-RS-calculated and NRTL-correlated mass fraction, respectively. The NRTL parameters and corresponding rmsds for the two DES systems are listed in Table 1. The estimated rmsds of ChCl/EG (1:2) and ChCl/Gly (1:2) systems are 0.0153 and 0.0180, respectively, indicating the high correlation accuracy of the NRTL model.

2.3.2. DES-Based Extraction Process. The process simulation for extracting *m*-cresol from cumene using DES as the extractant is carried out by Aspen Plus V11. The process flowsheet is shown in Figure 7. The DES and model coal tar are added to the top and bottom of the extraction column, respectively. After extraction, cumene is collected, and the *m*-cresol/DES mixture is delivered to the distillation column by a pump to recover the *m*-cresol and regenerate the DES. The product of *m*-cresol is obtained, while the regenerated DES is recycled through the cooler and valve into the mixer. Finally, a certain amount of fresh DES is fed to supplement the loss in process. In this DES-based extraction process, a sensitivity analysis is used to optimize the key operating conditions.

2.3.3. Extraction Process Analysis. The influences of the number of stages (NSs) on extraction performances of two DESs are shown in Figure S11 (Supporting Information). With the increase of the NS value, the cumene recovery ratio has no significant change, while the cumene mass purity and *m*-cresol recovery ratio increase evidently at first and then change slightly. For instance, for ChCl/EG (1:2), when the NS value rises from 2 to 6, the mass purity of cumene increases from 94.12 to 99.81%, while the recovery ratio of *m*-cresol increases from 86.50 to 99.68%, and the recovery ratio of cumene decreases slightly from 97.83 to 97.79%. When the NS value is further increased to 10, these values change hardly.

The influences of the mass-based solvent-to-feed ratio (S/F) on extraction performances of two DESs are given in Figure S12 (Supporting Information). As the S/F value increases gradually, more *m*-cresol in model coal tar is extracted into the DES. This can enhance cumene mass purity and increase the *m*-cresol recovery ratio. However, the cumene recovery ratio decreases with increasing S/F value. This is because more extractants lead to the simultaneous increase of the extraction capacity of *m*-cresol and cumene.

In order to gain a high cumene of at least of 0.999 and a high *m*-cresol recovery ratio of at least of 0.999 at the same time,[S3] the required NS value and the corresponding S/F value for two DESs are presented in Figure 8a. As is seen, the required S/F value reduces evidently at first and then reduces slightly with increasing NS value. For example, for ChCl/EG (1:2) and ChCl/Gly (1:2), the required S/F ratios are 1.55 and 1.07 at 2 stages, respectively, which reduce evidently to 0.46 and 0.29 at 8 stages, respectively, and reduce slightly to 0.45 and 0.27 at 10 stages, respectively. The reason may be that more stages enable more *m*-cresol to be extracted into the DES phase, thus decreasing the required DES. Furthermore, the cumene recovery ratio in the corresponding operating conditions of two DESs is depicted in Figure 8b. With the same NS value, the required S/F value of ChCl/Gly (1:2) is lower than that of ChCl/EG (1:2), while the cumene recovery ratio of ChCl/Gly

https://doi.org/10.1021/acsomega.2c04234
ACS Omega 2022, 7, 34485−34494

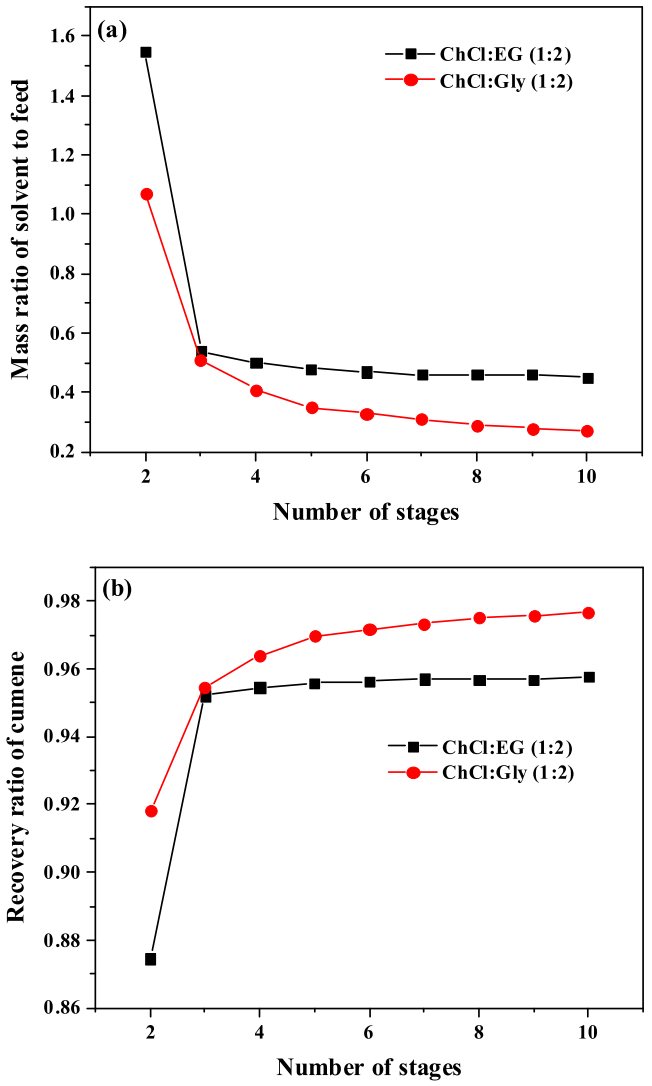

Figure 8. (a) S/F value as a function of the NS value in the extraction column; (b) cumene recovery ratio in the corresponding NS value and S/F value.

(1:2) is higher than that of ChCl/EG (1:2). These results indicate that ChCl/Gly (1:2) demonstrates better process performance than ChCl/EG (1:2). In summary, the NS value for the extraction column is selected as 8. The S/F values of ChCl/EG (1:2) and ChCl/Gly (1:2) are selected as 0.46 and 0.29, respectively.

2.3.4. Main Process Simulation Results. The regeneration process analyses of DESs are shown in Figures S13−S15 (Supporting Information). With the optimized operating conditions, a continuous extraction process for extracting *m*-cresol from cumene is simulated. The optimized operating conditions, the cumene and *m*-cresol products mass purities, as well as their recovery ratios, are listed in Table 2. The detailed simulation results of each stream are listed in Table S4 (Supporting Information). The feed of ChCl/Gly (1:2) is lower than that of ChCl/EG (1:2), while NS and reflux ratio (RR) values of ChCl/Gly (1:2) are significantly lower than those of ChCl/EG (1:2). The makeup values of ChCl/EG (1:2) and ChCl/Gly (1:2) are 1.36 and 2.99 kg·h^{-1}, respectively, indicating that the consumption of ChCl/Gly (1:2) is slightly higher than ChCl/EG (1:2) in the continuous process. Furthermore, both cumene mass purity and *m*-cresol recovery ratio for two DESs are greater than 0.999. The cumene recovery ratio and *m*-cresol mass purity of ChCl/Gly (1:2) are 0.9750 and 0.9448, respectively, and their values are higher than those of ChCl/EG (1:2) (0.9569 and 0.9085). The process simulation results are consistent with COSMO-RS calculations and extraction experiments. Based on the above-mentioned discussions, compared with ChCl/EG (1:2), ChCl/Gly (1:2) is a more promising DES in the extraction process for extracting *m*-cresol from cumene in the perspective of industrial application.

3. CONCLUSIONS

In this study, a multiscale method was presented and applied to screen DESs for extracting *m*-cresol from model coal tar. First, the effects of HBA and HBD compositions on DES extraction performances were investigated by COSMO-RS based on the molecular scale. ChCl/EG (1:2) and ChCl/Gly (1:2) were primarily selected as suitable extractants because they demonstrated high extraction performance at specific feed compositions derived from the mass-based LLE calculation. Then, the high performance of two DESs was confirmed by extraction experiments based on the single-stage equilibrium scale. Moreover, the extraction mechanism of DESs was studied through FT-IR characterization, indicating that DES and *m*-cresol can form a hydrogen bond. Finally, continuous process simulation based on the engineering scale was used to identify more promising DESs. Compared with ChCl/EG (1:2), ChCl/Gly (1:2) as the extractant could obtain higher mass purity and a higher recovery ratio of *m*-cresol and cumene products, as well as lower cost, indicating that ChCl/Gly (1:2) is a more promising DES in the extraction process. Overall, compared with extraction experiments alone, this multiscale method can quickly screen promising DESs in industrial applications.

4. METHOD DESCRIPTION

4.1. Phase Equilibrium Calculation by COSMO-RS. In this study, the phase equilibrium calculations of various DESs were carried out by BP_TZVP_18 parametrization in COSMOthermX software.[54] The σ-profiles of CCh, TEPC, Bu, and LA were obtained from quantum mechanical calculation. The structures of these components were optimized using the TURBOMOLE software at the BP/def-TZVP level.[35] Then, their *.cosmo* files were added to the COSMOthermX database. The σ-profiles of other components were directly obtained from the standard database of the COSMOthermX software. The detailed theory of LLE

Table 2. Main Results of the DES-based Extraction Process Simulation

	extraction column (eight stages)		distillation column			cumene product		*m*-cresol product	
DES	makeup DES (kg·h^{-1})	recycled DES (kg·h^{-1})	RR	NS	FS	mass purity	recovery ratio	mass purity	recovery ratio
ChCl/EG (1:2)	1.36	4598.64	15	27	8	0.9994	0.9569	0.9085	0.9991
ChCl/Gly (1:2)	2.99	2897.01	0.3	8	4	0.9992	0.9750	0.9448	0.9991

https://doi.org/10.1021/acsomega.2c04234
ACS Omega 2022, 7, 34485−34494

calculations by COSMO-RS could be found in the previous literature.[40,41] Some previous studies showed that COSMO-RS demonstrated high accuracy for phase equilibrium calculations of DES-containing systems.[55−57] Besides, the electroneutral method was applied to describe DESs in COSMO-RS calculation.[35,39]

After the phase equilibrium calculation, the extraction performance of DESs at different feed compositions is determined by eqs 2−4[53,54]

$$E\ \% = (m_{m-\text{cresol}} - w^{R}_{m-\text{cresol}} \cdot m^{R})/m_{m-\text{cresol}} \times 100\% \quad (2)$$

$$N\ \% = (m_{\text{cumene}} - w^{R}_{\text{cumene}} \cdot m^{R})/m_{\text{cumene}} \times 100\% \quad (3)$$

$$MR = w^{E}_{\text{cumene}}/w^{E}_{m-\text{cresol}} \quad (4)$$

where E, N, and MR represent extraction efficiency of m-cresol, entrainment of cumene, and mass ratio of cumene to m-cresol in the DES phase, respectively, m and w are the feed mass and mass fraction, respectively, and the superscript R and E refer to the raffinate phase and extract phase, respectively.

4.2. Experiments. The details of chemicals employed are shown in Table S5 (Supporting Information). All chemicals were used directly without further purification.

Certain quality HBA and HBD were added to a screw-capped vial. The HBA and HBD were mixed in a water bath at 348.15 K for 1 h (HWCL-3 within ±0.1 K, China). The DES was synthesized after spontaneously cooling to room temperature. The m-cresol + cumene mixture was prepared as model coal tar.

The extraction experiments were carried out as follows: 10.0 g of model coal tar was put into a 50 mL vial. An equal mass of DES was put into the model coal tar. The mixture was magnetically stirred for 2 h and settled for 45 min, and the water bath temperature was set at 298.15 K. Then, two phases were formed, and an analytical balance was used to weigh the mass of raffinate phase after it was removed from the extract phase by a separating funnel.

The composition of the raffinate phase was detected by gas chromatography (GC). The detailed analysis conditions are demonstrated in Table S6 (Supporting Information). The E, N, and MR values determined experimentally were also calculated by eqs 2−4. To investigate the extraction mechanism, m-cresol, DESs, and their mixtures were characterized by FT-IR (Thermo Scientific Nicolet iS50, USA).

■ ASSOCIATED CONTENT

Supporting Information

The Supporting Information is available free of charge at https://pubs.acs.org/doi/10.1021/acsomega.2c04234.

Details of selected HBAs and HBDs; COSMO-RS-calculated E, N, and MR of different DESs; σ-profile of nine HBDs; experimental and COSMO-RS-calculated MR of DESs; σ-potential of m-cresol, cumene, and DESs; required parameters for defining DESs into Aspen Plus; COSMO-RS-calculated and NRTL-correlated LLE data of {DES + m-cresol + cumene} ternary systems; sensitivity analysis of the extraction column and distillation column; detailed simulation results; chemicals used in this experiment; and detailed analysis conditions of GC (PDF)

■ AUTHOR INFORMATION

Corresponding Author

Xianglan Zhang − *School of Chemical and Environmental Engineering, China University of Mining and Technology (Beijing), Beijing 100083, China;* orcid.org/0000-0001-5435-1285; Email: zhxlcumtb@163.com

Author

Qian Liu − *School of Chemical and Environmental Engineering, China University of Mining and Technology (Beijing), Beijing 100083, China*

Complete contact information is available at: https://pubs.acs.org/10.1021/acsomega.2c04234

Notes

The authors declare no competing financial interest.

■ ACKNOWLEDGMENTS

The authors thank the National Key Research and Development Program of China (2016YFB0600305) for providing financial support.

■ ABBREVIATIONS

DESs	deep eutectic solvents
ILs	ionic liquids
HBA	hydrogen bond acceptor
HBD	hydrogen bond donor
LTCT	low-temperature coal tar
EDS	extractive desulfurization
FT-IR	Fourier transform infrared
UNIFAC	universal quasichemical functional−group activity coefficients
COSMO-RS	conductor-like screening model for real solvents
NRTL	non-random two liquids
LLE	liquid−liquid equilibrium
rmsd	root-mean-square deviation
GC	gas chromatography
E	extraction efficiency
N	neutral oil entrainment
MR	mass ratio of cumene to m-cresol
ChCl	choline chloride
ChBr	choline bromide
CChC	chlorocholine chloride
ATCC	acetylcholine chloride
TMAC	tetramethylammonium chloride
TEAC	tetraethylammonium chloride
TPAC	tetrapropylammonium chloride
TEAB	tetraethylammonium bromide
TEPC	tetraethylphosphonium chloride
EG	ethylene glycol
Gly	glycerol
Bu	1,2-butanediol
PA	benzyl alcohol
DEG	diethylene glycol
ET	monoethanolamine
AA	acetic acid
LA	lactic acid
OA	oxalic acid
NS	number of stages
S/F	solvent-to-feed ratio
FS	feed stage
RR	reflux ratio

https://doi.org/10.1021/acsomega.2c04234
ACS Omega 2022, 7, 34485−34494

REFERENCES

(1) Zhang, T.; Bing, X.; Wang, D.; Gao, J.; Zhang, L.; Xu, D.; Zhang, Y.; Wang, Y. Extraction and multi-scale mechanism explorations for separating indole from coal tar via tetramethylguanidine-based ionic liquids. *J. Environ. Chem. Eng.* **2021**, *9*, 105255.

(2) Ji, Y.; Hou, Y.; Ren, S.; Yao, C.; Wu, W. Separation of phenolic compounds from oil mixtures using environmentally benign biological reagents based on Brønsted acid-Lewis base interaction. *Fuel* **2019**, *239*, 926−934.

(3) Ma, S.; Yu, Q.; Hou, Y.; Li, J.; Li, Y.; Ma, Z.; Sun, L. Screening monoethanolamine as solvent to extract phenols from alkane. *Energy Fuel.* **2017**, *31*, 12997−13009.

(4) Xu, X.; Li, F.; Al-Haimi, A. A. N. M.; Ma, Y.; Zhang, L.; Xu, D.; Gao, J.; Wang, Y. Extraction performance evaluation and theoretical analysis of removal of phenol from oil mixture using a dual-functionalized ionic liquid: 1-hydroxyethyl-3-methylimidazolium propionate. *J. Chem. Technol. Biotechnol.* **2021**, *96*, 1947−1953.

(5) Xu, D.; Wang, S.; Zhang, T.; Peng, L.; Bing, X.; Zhang, L.; Ma, Y.; Gao, J.; Wang, Y. Extraction and interaction insights for enhanced separation of phenolic compounds from model coal tar using a hydroxyl-functionalized ionic liquid. *Chem. Eng. Res. Des.* **2022**, *178*, 567−574.

(6) Gai, H.; Qiao, L.; Zhong, C.; Zhang, X.; Xiao, M.; Song, H. A solvent based separation method for phenolic compounds from low-temperature coal tar. *J. Clean. Prod.* **2019**, *223*, 1−11.

(7) Liu, X.; Zhang, X. Solvent screening and liquid-liquid measurement for extraction of phenols from aromatic hydrocarbon mixtures. *J. Chem. Thermodyn.* **2019**, *129*, 12−21.

(8) Jiao, T.; Gong, M.; Zhuang, X.; Li, C.; Zhang, S. A new separation method for phenolic compounds from low-temperature coal tar with urea by complex formation. *J. Ind. Eng. Chem.* **2015**, *29*, 344−348.

(9) Hou, Y.; Ren, Y.; Peng, W.; Ren, S.; Wu, W. Separation of phenols from oil using imidazolium-based ionic liquids. *Ind. Eng. Chem. Res.* **2013**, *52*, 18071−18075.

(10) Yao, C.; Hou, Y.; Ren, S.; Ji, Y.; Wu, W.; Liu, H. Efficient separation of phenolic compounds from model oils by dual-functionalized ionic liquids. *Chem. Eng. Process.* **2018**, *128*, 216−222.

(11) Li, A.; Xu, X.; Zhang, L.; Gao, J.; Xu, D.; Wang, Y. Separation of cresol from coal tar by imidazolium-based ionic liquid [Emim]-[SCN]: Interaction exploration and extraction experiment. *Fuel* **2020**, *264*, 116908.

(12) Xu, D.; Zhong, P.; Peng, L.; Bing, X.; Yan, K.; Gao, J.; Zhao, P.; Zhang, L.; Wang, Y. Multiscale evaluation of the efficiently separation of phenols using a designed cationic functionalized ionic liquid based on Brønsted/Lewis coordination. *J. Mol. Liq.* **2022**, *345*, 117901.

(13) Xu, X.; Li, A.; Zhang, T.; Zhang, L.; Xu, D.; Gao, J.; Wang, Y. Efficient extraction of phenol from low-temperature coal tar model oil via imidazolium-based ionic liquid and mechanism analysis. *J. Mol. Liq.* **2020**, *306*, 112911.

(14) Ji, Y.; Hou, Y.; Ren, S.; Yao, C.; Wu, W. Highly efficient separation of phenolic compounds from oil mixtures by imidazolium-based dicationic ionic liquids via forming deep eutectic solvents. *Energy Fuel.* **2017**, *31*, 10274−10282.

(15) Yao, C.; Hou, Y.; Ren, S.; Wu, W.; Zhang, K.; Ji, Y.; Liu, H. Efficient separation of phenol from model oils using environmentally benign quaternary ammonium-based zwitterions via forming deep eutectic solvents. *Chem. Eng. J.* **2017**, *326*, 620−626.

(16) Yao, C.; Hou, Y.; Ren, S.; Wu, W.; Ji, Y.; Liu, H. Sulfonate based zwitterions: A new class of extractants for separating phenols from oils with high efficiency via forming deep eutectic solvents. *Fuel Process. Technol.* **2018**, *178*, 206−212.

(17) Li, G.; Xie, Q.; Liu, Q.; Liu, J.; Wan, C.; Liang, D.; Zhang, H. Separation of phenolic compounds from oil mixtures by betaine-based deep eutectic solvents. *Asia-Pac. J. Chem. Eng.* **2020**, *15*, No. e2515.

(18) Jiao, T.; Qin, X.; Zhang, H.; Zhang, W.; Zhang, Y.; Liang, P. Separation of phenol and pyridine from coal tar via liquid−liquid extraction using deep eutectic solvents. *Chem. Eng. Res. Des.* **2019**, *145*, 112−121.

(19) Li, G.; Xie, Q.; Ren, G.; Liu, J.; Liang, D. Mass transfer kinetics during the extraction of m-cresol from model coal tar using betaine/glycerol deep eutectic solvents. *Chem. Eng. Res. Des.* **2022**, *177*, 732−740.

(20) Yi, L.; Feng, J.; Li, W.; Luo, Z. High-performance separation of phenolic compounds from coal-based liquid oil by deep eutectic solvents. *ACS Sustainable Chem. Eng.* **2019**, *7*, 7777−7783.

(21) Hadj-Kali, M. K.; Mulyono, S.; Hizaddin, H. F.; Wazeer, I.; El-Blidi, L.; Ali, E.; Hashim, M. A.; AlNashef, I. M. Removal of thiophene from mixtures with *n*-heptane by selective extraction using deep eutectic solvents. *Ind. Eng. Chem. Res.* **2016**, *55*, 8415−8423.

(22) Wang, J.; Cheng, H.; Song, Z.; Chen, L.; Deng, L.; Qi, Z. Carbon dioxide solubility in phosphonium-based deep eutectic solvents: An experimental and molecular dynamics study. *Ind. Eng. Chem. Res.* **2019**, *58*, 17514−17523.

(23) Hizaddin, H. F.; Hadj-Kali, M. K.; Ramalingam, A.; Ali Hashim, M. A. Extractive denitrogenation of diesel fuel using ammonium- and phosphonium-based deep eutectic solvents. *J. Chem. Thermodyn.* **2016**, *95*, 164−173.

(24) Lei, Z.; Zhang, J.; Li, Q.; Chen, B. UNIFAC model for ionic liquids. *Ind. Eng. Chem. Res.* **2009**, *48*, 2697−2704.

(25) Chen, G.; Song, Z.; Qi, Z.; Sundmacher, K. Neural recommender system for the activity coefficient prediction and UNIFAC model extension of ionic liquid-solute systems. *AIChE J.* **2021**, *67*, No. e17171.

(26) Su, Y.; Wang, Z.; Jin, S.; Shen, W.; Ren, J.; Eden, M. R. An architecture of deep learning in QSPR modeling for the prediction of critical properties using molecular signatures. *AIChE J.* **2019**, *65*, No. e16678.

(27) Wen, H.; Su, Y.; Wang, Z.; Jin, S.; Ren, J.; Shen, W.; Eden, M. A systematic modeling methodology of deep neural network-based structure-property relationship for rapid and reliable prediction on flashpoints. *AIChE J.* **2022**, *68*, No. e17402.

(28) Zhang, J.; Wang, Q.; Su, Y.; Jin, S.; Ren, J.; Eden, M.; Shen, W. An accurate and interpretable deep learning model for environmental properties prediction using hybrid molecular representations. *AIChE J.* **2022**, *68*, No. e17634.

(29) Zhang, J.; Wang, Q.; Shen, W. Message-passing neural network based multi-task deep-learning framework for COSMO-SAC based σ-profile and V_{COSMO} prediction. *Chem. Eng. Sci.* **2022**, *254*, 117624.

(30) Klamt, A.; Eckert, F. COSMO-RS: a novel and efficient method for the a priori prediction of thermophysical data of liquids. *Fluid Phase Equil.* **2000**, *172*, 43−72.

(31) Eckert, F.; Klamt, A. Fast solvent screening via quantum chemistry: COSMO-RS approach. *AIChE J.* **2002**, *48*, 369−385.

(32) Liu, Q.; Bi, J.; Zhang, X. Effect of water on phenol separation from model oil with ionic liquids based on COSMO-RS calculation and experimental study. *ACS Omega* **2021**, *6*, 27368−27378.

(33) Dai, C.; Qi, Z.; Lei, Z.; Palomar, J. COSMO-based models. *Green Energy Environ.* **2021**, *6*, 309−310.

(34) Zhang, C.; Wu, J.; Wang, R.; Ma, E.; Wu, L.; Bai, J.; Wang, J. Study of the toluene absorption capacity and mechanism of ionic liquids using COSMO-RS prediction and experimental verification. *Green Energy Environ.* **2021**, *6*, 339−349.

(35) Hizaddin, H. F.; Ramalingam, A.; Hashim, M. A.; Hadj-Kali, M. K. O. Evaluating the performance of deep eutectic solvents for use in extractive denitrification of liquid fuels by the conductor-like screening model for real solvents. *J. Chem. Eng. Data* **2014**, *59*, 3470−3487.

(36) Salleh, Z.; Wazeer, I.; Mulyono, S.; El-blidi, L.; Hashim, M. A.; Hadj-Kali, M. K. Efficient removal of benzene from cyclohexane-benzene mixtures using deep eutectic solvents − COSMO-RS screening and experimental validation. *J. Chem. Thermodyn.* **2017**, *104*, 33−44.

(37) Hadj-Kali, M. K.; Hizaddin, H. F.; Wazeer, I.; El blidi, L.; Mulyono, S.; Hashim, M. A. Liquid-liquid separation of azeotropic mixtures of ethanol/alkanes using deep eutectic solvents: COSMO-RS prediction and experimental validation. *Fluid Phase Equil.* **2017**, *448*, 105−115.

https://doi.org/10.1021/acsomega.2c04234
ACS Omega 2022, 7, 34485−34494

(38) Song, Z.; Wang, J.; Sundmacher, K. Evaluation of COSMO-RS for solid−liquid equilibria prediction of binary eutectic solvent systems. *Green Energy Environ.* **2021**, *6*, 371−379.
(39) Qin, Z.; Cheng, H.; Song, Z.; Ji, L.; Chen, L.; Qi, Z. Selection of deep eutectic solvents for extractive deterpenation of lemon essential oil. *J. Mol. Liq.* **2022**, *350*, 118524.
(40) Song, Z.; Zhou, T.; Qi, Z.; Sundmacher, K. Systematic method for screening ionic liquids as extraction solvents exemplified by an extractive desulfurization process. *ACS Sustainable Chem. Eng.* **2017**, *5*, 3382−3389.
(41) Cheng, H.; Liu, C.; Zhang, J.; Chen, L.; Zhang, B.; Qi, Z. Screening deep eutectic solvents for extractive desulfurization of fuel based on COSMO-RS model. *Chem. Eng. Process.* **2018**, *125*, 246−252.
(42) Gai, H.; Qiao, L.; Zhong, C.; Zhang, X.; Xiao, M.; Song, H. Designing ionic liquids with dual lewis basic sites to efficiently separate phenolic compounds from low-temperature coal tar. *ACS Sustainable Chem. Eng.* **2018**, *6*, 10841−10850.
(43) Liu, Q.; Zhang, X.; Li, W. Separation of *m*-cresol from aromatic hydrocarbon and alkane using ionic liquids via hydrogen bond interaction. *Chin. J. Chem. Eng.* **2019**, *27*, 2675−2686.
(44) Bing, X.; Wang, Z.; Wei, F.; Gao, J.; Xu, D.; Zhang, L.; Wang, Y. Separation of *m*-cresol from coal tar model oil using propylamine-based ionic liquids: Extraction and interaction mechanism exploration. *ACS Omega* **2020**, *5*, 23090−23098.
(45) Gao, S.; Jin, J.; Abro, M.; He, M.; Chen, X. Selection of ionic liquid for extraction processes: Special case study of extractive desulfurization. *Chem. Eng. Res. Des.* **2021**, *167*, 63−72.
(46) Song, Z.; Zhang, C.; Qi, Z.; Zhou, T.; Sundmacher, K. Computer-aided design of ionic liquids as solvents for extractive desulfurization. *AIChE J.* **2018**, *64*, 1013−1025.
(47) Ji, Y.; Hou, Y.; Ren, S.; Yao, C.; Wu, W. Highly efficient extraction of phenolic compounds from oil mixtures by trimethylamine-based dicationic ionic liquids via forming deep eutectic solvents. *Fuel Process. Technol.* **2018**, *171*, 183−191.
(48) Huang, Y.; Dong, H.; Zhang, X.; Li, C.; Zhang, S. A new fragment contribution-corresponding states method for physicochemical properties prediction of ionic liquids. *AIChE J.* **2013**, *59*, 1348−1359.
(49) Valderrama, J. O.; Robles, P. A. Critical properties, normal boiling temperatures and acentric factors of fifty ionic liquids. *Ind. Eng. Chem. Res.* **2007**, *46*, 1338−1344.
(50) Mirza, N. R.; Nicholas, N. J.; Wu, Y.; Kentish, S.; Stevens, G. W. Estimation of normal boiling temperatures, critical properties, and acentric factors of deep eutectic solvents. *J. Chem. Eng. Data* **2015**, *60*, 1844−1854.
(51) Wu, Z.; Zeng, Q.; Cheng, H.; Chen, L.; Qi, Z. Extractive separation of tetralin-dodecane mixture using tetrabutylphosphonium bromide-based deep eutectic solvent. *Chem. Eng. Process.* **2020**, *149*, 107822.
(52) Ma, S.; Hou, Y.; Sun, Y.; Li, J.; Li, Y.; Sun, L. Simulation and experiment for ethanol dehydration using low transition temperature mixtures (LTTMs) as entrainers. *Chem. Eng. Process.* **2017**, *121*, 71−80.
(53) Liu, Q.; Zhang, X. Systematic method of screening deep eutectic solvents as extractive solvents for *m*-cresol/cumene separation. *Sep. Purif. Technol.* **2022**, *291*, 120853.
(54) Liu, Q.; Zhang, X. Highly efficient separation of phenolic compounds from low-temperature coal tar by composite extractants with low viscosity. *J. Mol. Liq.* **2022**, *360*, 119417.
(55) Gouveia, A. S. L.; Oliveira, F. S.; Kurnia, K. A.; Marrucho, I. M. Deep eutectic solvents as azeotrope breakers: liquid-liquid extraction and COSMO-RS prediction. *ACS Sustainable Chem. Eng.* **2016**, *4*, 5640−5650.
(56) Mulyono, S.; Hizaddin, H. F.; Wazeer, I.; Alqusair, O.; Ali, E.; Ali Hashim, M. A.; Hadj-Kali, M. K. Liquid-liquid equilibria data for the separation of ethylbenzene/styrene mixtures using ammonium-based deep eutectic solvents. *J. Chem. Thermodyn.* **2019**, *135*, 296−304.
(57) Darwish, A. S.; Abu Hatab, F.; Lemaoui, T.; Ibrahim, O. A. Z.; Almustafa, G.; Zhuman, B.; Warrag, S. E. E.; Hadj-Kali, M. K.; Benguerba, Y.; Alnashef, I. M. Multicomponent extraction of aromatics and heteroaromatics from diesel using acidic eutectic solvents: Experimental and COSMO-RS predictions. *J. Mol. Liq.* **2021**, *336*, 116575.

https://doi.org/10.1021/acsomega.2c04234
ACS Omega 2022, 7, 34485−34494